Research Article | Vol. 9, No. 5 | 1 May 2018 | BIOMEDICAL OPTICS EXPRESS 2068
Biomedical Optics EXPRESS

Liquid phantoms for near-infrared and diffuse correlation spectroscopies with tunable optical and dynamic properties

LORENZO CORTESE,[1,8,*] GIUSEPPE LO PRESTI,[1,8] MARCO PAGLIAZZI,[1] DAVIDE CONTINI,[2] ALBERTO DALLA MORA,[2] ANTONIO PIFFERI,[2,3] SANATHANA KONUGOLU VENKATA SEKAR,[2] LORENZO SPINELLI,[3] PAOLA TARONI,[2,3] MARTA ZANOLETTI,[2] UDO M. WEIGEL,[4] SIXTE DE FRAGUIER,[5] AN NGUYEN-DIHN,[6] BOGDAN ROSINSKI,[6] AND TURGUT DURDURAN[1,7]

[1] *ICFO-Institut de Ciències Fotòniques, The Barcelona Institute of Science and Technology, 08860 Castelldefels (Barcelona), Spain*
[2] *Politecnico di Milano, Dipartimento di Fisica, 20133 Milano, Italy*
[3] *Istituto di Fotonica e Nanotecnologie, Consiglio Nazionale delle Ricerche, 20133 Milano, Italy*
[4] *HemoPhotonics S.L., 08860 Castelldefels (Barcelona), Spain*
[5] *ECM - ECHO CONTROL MEDICAL, S.A.S., 16000 Angoulême, France*
[6] *VERMON S.A., 37000 Tours, France*
[7] *Institució Catalana de Recerca i Estudis Avançats (ICREA), 08015 Barcelona, Spain*
[8] *These authors equally contributed to this work*
[*] *lorenzo.cortese@icfo.es*

Abstract: We present the recipe and characterization for preparing liquid phantoms that are suitable for both near-infrared spectroscopy and diffuse correlation spectroscopy. The phantoms have well-defined and tunable optical and dynamic properties, and consist of a solution of water and glycerol with fat emulsion as the scattering element. The recipe takes into account the effect of bulk refractive index changes due to the addition of glycerol, which is commonly used to alter the sample viscosity.

OCIS codes: (170.3660) Light propagation in tissues; (170.6480) Spectroscopy, speckle; (290.0290) Scattering; (290.1990) Diffusion.

References and links

1. T. Durduran, R. Choe, W. B. Baker, and A. G. Yodh, "Diffuse optics for tissue monitoring and tomography," Rep. Prog. Phys. **73**(7), 076701 (2010).
2. M. S. Patterson, B. Chance, and B. C. Wilson, "Time resolved reflectance and transmittance for the non-invasive measurement of tissue optical properties," Appl. Optics **28**, 2331 (1989).
3. S. Konugolu Venkata Sekar, I. Bargigia, A. Dalla Mora, P. Taroni, A. Ruggeri, A. Tosi, A. Pifferi, and A. Farina, "Diffuse optical characterization of collagen absorption from 500 to 1700 nm," J. Biomed. Opt. **22**(1), 015006 (2017).
4. D. A. Boas, L. E. Campbell, and A. G. Yodh, "Scattering and imaging with diffusing temporal field correlations," Phys. Rev. Lett. **75**, 1855–1858 (1995).
5. D. A. Boas, and A. G. Yodh, "Spatially varying dynamical properties of turbid media probed with diffusing temporal light correlation," J. Opt. Soc. Am. A **14**, 192–215 (1997)
6. D. Irwin, L. Dong, Y. Shang, R. Cheng, M. Kudrimoti, S. D. Stevens, and G. Yu, "Influences of tissue absorption and scattering on diffuse correlation spectroscopy blood flow measurements," Biomed. Opt. Express **2**(7), 1969–1985 (2011).
7. R. Cubeddu, A. Pifferi, P. Taroni, A. Torricelli, and G. Valentini, "A solid tissue phantom for photon migration studies," Phys. Med. Biol. **42**(10), 1971 (1997).
8. B. W. Pogue and M. S. Patterson, "Review of tissue simulating phantoms for optical spectroscopy, imaging and dosimetry," J. Biomed. Opt. **11**(4), 041102 (2006).
9. P. Di Ninni, F. Martelli, and G. Zaccanti, "Effect of dependent scattering on the optical properties of Intralipid tissue phantoms," Biomed. Opt. Express **2**(8), 2265–2278 (2011).

#321229 https://doi.org/10.1364/BOE.9.002068
Journal © 2018 Received 2 Feb 2018; revised 16 Mar 2018; accepted 19 Mar 2018; published 4 Apr 2018

Biomedical Optics EXPRESS

10. P. Di Ninni, F. Martelli, and G. Zaccanti, "Intralipid: towards a diffusive reference standard for optical tissue phantoms," Phys. Med. Biol. **56**(2), N21 (2011).
11. P. Di Ninni, Y. Bérubé-Lauzière, L. Mercatelli, E. Sani, and F. Martelli, "Fat emulsions as diffusive reference standards for tissue simulating phantoms?" Appl. Opt. **51**(30), 7176–7182 (2012).
12. H. J. van Staveren, C. J. M. Moes, J. van Marie, S. A. Prahl, and M. J. C. van Gemert, "Light scattering in Intralipid-10% in the wavelength range of 400-1100 nm," Appl. Opt. **30**(31), 4507–4514 (1991).
13. S. T. Flock, S. L. Jacques, B. C. Wilson, W. M. Star, and M. J. C. van Gemert, "Optical properties of Intralipid: a phantom medium for light propagation studies," Laser Surg. Med. **12**(5), 510–519 (1992).
14. L. A. Dempsey, M. Persad, S. Powell, D. Chitnis, and J. C. Hebden, "Geometrically complex 3D-printed phantoms for diffuse optical imaging," Biomed. Opt. Express **8**(3), 1754–1762 (2017).
15. D. A. Boas, S. Sakadžic, J. Selb, P. Farzam, M. A. Franceschini, and S. A. Carp.,"Establishing the diffuse correlation spectroscopy signal relationship with blood flow," Neurophotonics **3**(3), 031412 (2016).
16. L. Gagnon, M. Desjardins, J. Jehanne-Lacasse, L. Bherer, and F. Lesage, "Investigation of diffuse correlation spectroscopy in multi-layered media including the human head," Opt. Express **16**(20), 15514–15530 (2008).
17. D. A. Boas, "Diffuse photon probes of structural and dynamical properties of turbid media: theory and biomedical applications," PhD Dissertation, University of Pennsylvania (1996).
18. C. Cheung, J. P. Culver, K. Takahashi, J. H. Greenberg, and A. G. Yodh, "*In vivo* cerebrovascular measurement combining diffuse near-infrared absorption and correlation spectroscopies," Phys. Med. Biol. **46**(8), 2053 (2001).
19. Y. Lin, L. He, Y. Sang, G. Yu, "Noncontact diffuse correlation spectroscopy for noninvasive deep tissue blood flow measurement," J. Biomed. Opt. **17**(1), 010502 (2012).
20. H. S. Yazdi, T. D. O'Sullivan, A. Leproux, B. Hill, A. Durkin, S. Telep, J. Lam, S. S. Yadzi, A. M. Police, R. M. Carrol, F. J. Combs, T. Strömberg, A.G. Yodth, and B. Tromberg, "Mapping breast cancer blood flow index, composition, and metabolism in a human subject using combined diffuse optical spectroscopic imaging and diffuse correlation spectroscopy," J. Biomed. Opt. **22**(4), 045003 (2017)
21. J. Dong, R. Bi, J. Hui Ho, P. S. P. Thong, K.-C. Soo, and K. Leea, "Diffuse correlation spectroscopy with a fast Fourier transform-based software autocorrelator," J. Biomed. Opt. **17**(9), 097004 (2012).
22. J. Kim and H. Liu, "Investigation of biphasic tumor oxygen dynamics induced by hyperoxic gas intervention: the dynamic phantom approach," Appl. Opt. **47**(2), 242–252 (2008).
23. T. Binzoni, A. Torricelli, R. Giust, B. Sanguinetti, P. Bernhard, and L. Spinelli, "Bone tissue phantoms for optical flowmeters at large interoptode spacing generated by 3D-stereolithography," Biomed. Opt. Express **5**(8), 2715–2725 (2014).
24. J. P. O'Reilly, N. J. Kolodziejski, D. McAdams, D. E. Fernandez, C. J. Stapels, and J. F. Christian, "A capillary-mimicking optical tissue phantom for diffuse correlation spectroscopy," Proc. of SPIE **10056**, 1005613 (2017).
25. Glycerine Producers' Association, "Physical properties of glycerineand its solutions" (1963).
26. Lipofundin20% has been chosen due to its facility of being purchased in the region of ICFO, Barcelona. For differences between other initial concentrations (i. e. Lipofundin10%) and different lipid emulsions (Intralipid and Lipovenoes) we refer to the work of Di Ninni et al. [11].
27. L. Spinelli, M. Botwicz, N. Zolek, M. Kacprzak, D. Milej, P. Sawosz, A. Liebert, U. Weigel, T. Durduran, F. Foschum, A. Kienle, F. Baribeau, S. Leclair, J.-P. Bouchard, I. Noiseux, P. Gallant, O. Mermut, A. Farina, A. Pifferi, A. Torricelli, R. Cubeddu, H.-C. Ho, M. Mazurenka, H. Wabnitz, K. Klauenberg, O. Bodnar, C. Elster, M. Bénazech-Lavoué, Y. Bérubé-Lauzière, F. Lesage, D. Khoptyar, A. A. Subash, S. Andersson-Engels, P. Di Ninni, F. Martelli, and G. Zaccanti, "Determination of reference values for optical properties of liquid phantoms based on Intralipid and India ink," Biomed. Opt. Express **5**(7), 2037–2053 (2014).
28. F. Martelli, P. Di Ninni, G. Zaccanti, D. Contini, L. Spinelli, A. Torricelli, R. Cubeddu, H. Wabnitz, M. Mazurenka, R. MacDonald, A. Sassaroli, and A. Pifferi, "Phantoms for diffuse optical imaging based on totally absorbing objects, part 2: Experimental implementation," J. Biomed. Opt. **19**(7), 076011 (2014).
29. F. Martelli, S. Del Bianco, A. Ismaelli, and G. Zaccanti, '*Light Propagation through Biological Tissue and Other Diffusive Media: Theory, Solutions and Software* (SPIE, 2010).
30. R. Elaloufi, R. Carminati, and J.-J. Greffet, "Time-dependent transport through scattering media: from radiative transfer to diffusion," J. Opt. A - Pure Appl. Opt. **4**, S103–S108 (2002).
31. R. Elaloufi, R. Carminati, and J.-J. Greffet, "Diffusive-to-ballistic transition in dynamic light transmission through thin scattering slabs: a radiative transfer approach," J. Opt. Soc. Am. A **21**(8), 1430–1437 (2004).
32. R. Graaff, J. G. Aarnoose, J. R. Zijp, P. M. A. Sloot, F. F. M. de Mul, J. Greve, and M. H. Koelink, "Reduced light-scattering properties for mixtures of spherical particles: a simple approximation derived from Mie calculations," Appl. Opt. **31**, 1370–1376 (1992).
33. J. R. Mourant, T. Fuselier, J. Boyer, T. Johnson, and I. J. Bigio, "Predictions and measurements of scattering and absorption over broad wavelength ranges in tissue phantoms," Appl. Opt. **36**, 949–957 (1997).
34. S. Srinivasan, B. W. Pogue, S. Jiang, H. Dehghani, C. Kogel, S. Soho, J. G. Chambers, T. D. Tosteson, S. P. Poplack, and K. D. Paulsen, "Interpreting hemoglobin and water concentration, oxygen saturation, and scattering measured by near-infrared tomography of normal breast in vivo," PNAS **100**(21), 12349–12354 (2003).
35. A. Einstein, "Investigations on the Theory of the Brownian Movement," Dover Publications (1956) [Republication of the original 1926 translation].
36. S. Konugolu Venkata Sekar, A. Dalla Mora, I. Bargigia, E. Martinenghi, C. Lindner, P. Farzam, M. Pagliazzi, T.

Biomedical Optics EXPRESS

Durduran, P. Taroni, A. Pifferi, and Andrea Farina, "Broadband (600 - 1350 nm) time-resolved diffuse optical spectrometer for clinical use," IEEE J. of Sel. Top. Quant. **22**(3), 406–414 (2016).
37. C. Lindner, M. Mora, P. Farzam, M. Squarcia, J. Johansson, U. M. Weigel, I. Halperin, F. Hanzu, and T. Durduran, "Diffuse optical characterization of the healthy human thyroid tissue and two pathological case studies," PloS One **11**(1), e0147851 (2016).
38. L. Spinelli, F. Martelli, A. Farina, A. Pifferi, A. Torricelli, R. Cubeddu, and G. Zaccanti, "Calibration of scattering and absorption properties of a liquid diffusive medium at NIR wavelengths. Time-resolved method," Opt. express **15**(11), 6589–6604 (2007).
39. S. L. Jacques, "Optical properties of biological tissues: a review," Phys. Med. Biol. **58**, R37–R61 (2013).

1. Introduction

The combination of diffuse correlation spectroscopy (DCS) with near-infrared diffuse optical spectroscopy (NIRS) provides important and complementary information about the composition, structure and hemodynamics of the tissue under investigation [1]. Therefore, recently this combination has gained popularity as an emerging non-invasive biomedical modality. NIRS methods like time-resolved spectroscopy (TRS), frequency-domain or continuous wave optical spectroscopy allow the quantification of the wavelength dependent optical absorption and scattering coefficients of the probed tissue which, in turn, permit the estimation of the concentration of chromophores like oxy- and deoxy-haemoglobin, water, lipids, collagen, and give information on cell structure [2, 3]. Near-infrared diffuse correlation spectroscopy (DCS), on the other hand, exploits the decay of the diffuse intensity auto-correlation function due to altered speckle statistics coming from diffuse light by moving particles (primarily red blood cells) in order to measure the microvascular blood flow in the tissue [1, 4, 5]. By combining the information retrieved by NIRS and DCS, it is possible to enhance the sensitivity to the hemodynamic biomarkers in order to discriminate between healthy and different pathological conditions such as brain injury, malignancy and others. Furthermore, the combination of NIRS and DCS increases the precision in retrieving the blood flow index by fixing parameters such as the reduced scattering coefficient and the absorption coefficient in DCS fitting procedure [1, 6].

In order to validate and standardize NIRS and DCS measurements for clinical applications, it is important to develop reference standard phantoms, i.e. systems that mimic and reproduce the optical and dynamic properties of the tissue. Phantoms with calibrated properties are used to develop the system at the laboratory level, to measure the system performances against standardized protocols, to allow daily quality checks in clinical studies and to calibrate instruments for absolute measurements. All these measures go in the direction of increasing the reliability, and reproducibility of clinical studies and also to set the floor for standardization activities in the field [7, 8].

The design of phantoms for NIRS allows their preparation with well-controllable optical properties. Essentially, the ideal bulk medium is non-diffusive and transparent in the whole optical spectrum of interest with the possibility to add the scattering centers and the absorbing centers in the proper ratio so as to obtain the desired wavelength (λ) dependent absorption coefficient ($\mu_a(\lambda)$) and reduced scattering coefficient ($\mu_s'(\lambda)$). In literature we find several examples of liquid phantoms made of suspension of small fat droplets in water (lipid emulsions such as Intralipid20% - Fresenius Kaby, Germany -, Lipofundin20% - B. Braun Melsungen AG, Germany, and many others) and ink [9–13], and, solid phantoms made of epoxy resin or silicon rubber and titanium dioxide particles as scatterers [7, 8, 14].

The requirements of a phantom for DCS are basically the same as those of NIRS but with some additional constraints. The main difference is that DCS is based on the measurement of the temporal auto-correlation of laser speckles in the turbid medium which depends on the motion of the scattering centers. We note that it has been observed that the decay of the temporal autocorrelation curves of diffuse photons emerging from tissue is well fitted using an effective particle Brownian motion model [1, 15]. Therefore, DCS phantoms often use the Brownian motion

Biomedical Optics EXPRESS

of the scattering centers as a contrast factor. Most common DCS phantoms are liquid phantoms made of water and Intralipid20% or Lipofundin20%. Previous attempts in changing the particle Brownian motion coefficient (D_b) varied from changing the viscosity of the medium to changing the temperature or inducing forced motion by pumps [16–24]. However, all these methods present different challenges that, to date, have not been addressed thoroughly. Viscosity is often altered by mixing glycerol or methyl-cellulose which alter also the index of refraction of the bulk medium hence altering light scattering properties [25]. Temperature also changes the viscosity of the bulk medium (often water) and may alter the composition of the fat droplets. Finally, forced motion induced by pumps through pipes or porous materials may lead to unpredictable dynamics.

Here, we demonstrate a recipe to fabricate a liquid phantom for near infrared spectroscopy and diffuse correlation spectroscopy with well-defined optical (absorption and scattering) and dynamic (Brownian diffusion coefficient) properties considering solutions of water and glycerol with Lipofundin20% (B. Braun Melsungen AG, DE) as the scattering element while accounting for the bulk refractive index changes. The dynamic and scattering properties of the phantoms can be tuned considering that the motion of the scatterers depends on the relative concentration of glycerol in water, which alters the viscosity of the solution, and that the reduced scattering coefficient of the system depends both on the concentration of scatterers and glycerol in the solution [25]. In the next sections we present the outcomes of independent TRS characterization experiments and of DCS experiments to develop this recipe.

2. Materials and methods

2.1. Phantoms

The phantoms considered for this study are solutions of ultrapure (Milli-Q, Milipore, USA) water and glycerol (Sigma-Aldrich Co. LLC. U.S., cod. 49770, ≥ 99.5%) with Lipofundin20% (B. Braun Melsungen AG, DE) [26] as the scattering element. We have mixed phantoms with different concentrations of glycerol in water ranging from 0% to 30% of the solution. For each concentration of glycerol, we have changed the concentration of scatterers ranging from 0.1% to approximately 4.0% of the solution by sequentially adding Lipofundin20% (mixed with glycerol, in order to preserve the ratio between water and glycerol). In this study, we have decided to not change the absorption of the phantoms, since, as shown in several works and as reported in the following sections, the absorption coefficient can be tuned independently from the scattering and dynamic properties by adding ink or other absorbers to the solution [27]. The experiments on every single phantom have been performed during one single day of measurements. For this reason, based on previous studies [10] and our experience, the optical and dynamic properties of the phantoms used can be considered stable over the duration of the experiments.

Experiments were conducted at two sites - Politecnico di Milano (POLIMI, Milan, Italy) and ICFO-the Institute of Photonic Sciences (ICFO, Barcelona, Spain). For the experiments performed at POLIMI, we have prepared solutions of 0%, 5%, 10%, 15%, 20%, 25%, 30% of glycerol in Milli-Q water. For each different solution of water and glycerol, the scatterer concentration is varied between 0.1% and 1.2% of the whole solution in ten equally spaced steps. The liquid solutions have been placed in a black PVC phantom box. The frontal wall of the phantom box has small transparent windows, allowing the laser light to enter the diffusive medium, and the re-emitted photons to be collected outside the box. The top of the phantom box is exposed to the air and the whole set is covered by a dark, light-proof curtain during the experiments. More details about the phantom box can be found in Ref. [28].

For the two independent experiments performed at ICFO, we have prepared solutions of 0%, 20% and 30% of glycerol in Milli-Q water. In order to obtain roughly similar scattering coefficient (considering that higher concentrations of glycerol reduces the scattering strength), we have added different concentrations of scatterers in the three phantoms with different glycerol concentration; for the phantom with 0% of glycerol, we have considered 0.75%, 1.5% and 2.3%

Biomedical Optics EXPRESS

concentrations of scatterers, for the phantom with 20% of glycerol, we have considered 0.89%, 1.8% and 2.7% concentrations of scatterers, and finally, for the phantom with 30% of glycerol, we have considered 1.3%, 2.6% and 4.0% concentrations of scatterers. The solutions that were placed in a black phantom box with a size of 20 $cm \times 20\ cm \times 20\ cm$ which allow the access of the optical fibers used for the experiments from the top side of the box. The top of the phantom box is exposed to the air and the whole set is covered by a dark, light-proof curtain during the experiments.

2.2. Physical model

2.2.1. Scattering properties

The optical properties of a liquid phantom are strongly dependent on several parameters such as the concentration of the scatterers, the refractive index contrast between the scattering elements and the environment and the wavelength of the light. In the independent scattering regime (low concentration of scatterers, each scattering event can be considered independent from the previous events), for a fixed wavelength λ, the bulk reduced scattering coefficient μ_s' of the phantoms is directly linked to the concentration of the scattering elements and to the scattering properties of a single scatterer through the relation [29]

$$\mu_s'(\lambda) = \rho_s (1 - g)\, \sigma_s, \tag{1}$$

where σ_s is the scattering cross section, g is the anisotropy factor and ρ_s is the concentration of the scatterers. For a fixed solution of glycerol and water, the reduced scattering coefficient of the system linearly increases with the concentration of scatterers. For practical purposes, in order to interpret the experimental results, equation 1 is commonly reduced to the relation

$$\mu_s'(\lambda) = \epsilon_s \rho_s + C, \tag{2}$$

where ϵ_s is the 'intrinsic' reduced scattering coefficient of the scattering element and C is a coefficient accounting for the fact that diffusion theory does not work properly for low concentration of scatterers [29–31].

Moreover, the reduced scattering coefficient depends on the refractive index contrast between scatterers and the bulk medium. For this reason, considering scatterers with higher refractive index than the bulk medium, it is expected that the reduced scattering coefficient decreases when the glycerol concentration in water increases. Adding glycerol (refractive index $n = 1.47$) to water ($n = 1.33$), indeed, reduces the refracting index contrast between scatterers and environment which affect the scattering cross section σ_s and the anisotropy factor g in equation 1. As described by the Mie theory of light scattering, the decrease of the reduced scattering coefficient for increasing glycerol concentration ρ_{glyc} is expected to be linear, given by

$$\epsilon_s(\lambda) = \epsilon_{glyc} \rho_{glyc} + \epsilon_s^0, \tag{3}$$

where ϵ_s is the 'intrinsic' scattering coefficient of the scattering element, ϵ_{glyc} is the proportional coefficient depending on the optical properties of glycerol, and ϵ_s^0 is the intrinsic reduced scattering coefficient of Lipofundin in water (0% of glycerol).

The optical properties of a liquid phantom are strongly dependent on the wavelength (λ) of the light. For tissue simulating phantoms in the near-infrared region, the dependence of the intrinsic reduced scattering coefficient, ϵ_s, on the wavelength, λ, is well described by the power law derived from Mie scattering theory [8, 12, 13, 32–34]

$$\epsilon_s(\lambda) = A \left(\frac{\lambda}{\lambda_0} \right)^{-b}, \tag{4}$$

where A and b are related mainly to the density and refractive index contrast, and size of the scattering centers respectively, while λ_0 is a reference wavelength.

Biomedical Optics EXPRESS

Dynamic properties The dynamic properties of a liquid phantom can be controlled by changing the viscosity of the solution in which the scatterers are suspended. The Brownian diffusion coefficient D_b of a particle undergoing Brownian motion in a fluid depends indeed on the viscosity η of the solution, following the Einstein relation [35]

$$D_b = \frac{K_B}{6\pi}\frac{T}{r\,\eta}, \tag{5}$$

where K_B is the Boltzmann's constant, T is the temperature and r is the radius of the particle. This relation states that, in the same environmental conditions, the ratio between the D_b related to particles in two solutions with different viscosity is equal to the inverse of the ratio of the viscosity of the solutions

$$\frac{D_{b1}}{D_{b2}} = \frac{\eta_2}{\eta_1}. \tag{6}$$

2.3. Experimental setup and analysis method

2.3.1. Politecnico di Milano (POLIMI) experiments

The time-resolved spectroscopy experiments carried on in *Politecnico di Milano* have been performed with the broadband time-resolved diffuse optical spectrometer described in ref. [36]. The system consists of broadband ($450 - 1750$ *nm*) fiber laser with a 60 MHz repetition rate. A pellin broca prism couples the selected wavelength into a 50 μm fiber. Depending on the selected wavelength, the power at the tip of source fiber varies between 0.5 to 6 mW. Detection is achieved by a multi-mode step index fiber (1 *mm* core, length 50 *cm*, NA 0.39) connected to a photomultiplier tube (double channel microchannel plate). A time correlated single photon counting card (SPC-130, Becker & Hickl GmbH, Germany) was utilized for the acquisition of temporal curves. In this study, the measurements were performed in reflectance geometry at two source detector separations 20 and 30 *mm*, and, at six wavelengths 600, 700, 785, 900, 1000 and 1100 *nm*.

The reduced scattering coefficients at the wavelengths of 600, 700 and 785 *nm* were retrieved by exploiting a linear method comparing the distribution of time of flights of photons at two different source-detector separations as described in ref. [38]. The linear method gives reliable results for the reduced scattering only in the diffusive regime and, therefore, it was not applied at measurements performed at wavelengths 900, 1000 and 1100 *nm* where the values of the reduced scattering coefficient were too low. The absorption coefficients have, on the other hand, been retrieved for all the wavelengths by a non-linear fit of the solution of the diffusion equation for a homogeneous medium, convoluted with the instrument response function as described in the following Section. The measurements have been performed at a room temperature of (25 ± 2) °C.

2.3.2. The Institute of Photonic Sciences experiments

Diffuse correlation spectroscopy and time-resolved spectroscopy experiments carried on at *ICFO* have been performed with a single hybrid diffuse optical device [37]. The DCS module of the hybrid device consists in single longitudinal mode laser (DL785-120-SO, CrystaLaser, Reno, NV, USA) as source. Light is injected in the phantom using a 200 μm core multimode fiber and the diffused reflectance is collected using a fiber bundle consisting of four 5.6 μm core single mode fibers. The detection part consists of four single photon counting avalanche photodiodes (SPCM-AQ4C, Excelitas, Québec, Canada), and the intensity temporal autocorrelation function of each channel is calculated in real time by a 8-channel digital correlator (correlator.com, New Jersey, USA). Source and detection fibers are placed in reflectance geometry at a distance of 2.5 *cm*. The acquired intensity temporal autocorrelation functions (g_2) are transformed into electric field temporal autocorrelation functions (g_1) which are fitted with the solution of the correlation diffusion equation for a semi-infinite medium (with extrapolated boundary

Biomedical Optics EXPRESS

conditions), as reported in ref. [1], in order to retrieve the scatterer Brownian diffusion coefficient (D_b). In the fitting procedure, we have considered the properly weighted index of refraction of solutions of water and glycerol, reported in literature [25]. Moreover, the absorption and reduced scattering coefficients (μ_a and μ_s') are fixed parameters determined through the TRS measurements performed on the very same phantoms.

The TRS part used one pulsed laser (BHLP-700, Becker & Hickl GmbH, Germany) with a repetition rate of 50 MHz and wavelength 785 nm. The laser light is sent to the phantom through a 62.5 μm core graded index fiber and the diffused reflectance is collected using a 54 fiber bundle of 62.5 μm core graded index fibers. The detection part consists of a hybrid photomultiplier detector (HPM-100-50, Becker & Hickl GmbH, Berlin, Germany) connected to a time correlated single photon counting card (SPC-130, Becker & Hickl GmbH, Berlin, Germany) and a detector control card (DCC-100, Becker & Hickl GmbH, Berlin, Germany).

We have acquired the distribution of time of flights of photons (DTOF) in reflectance geometry for a source-detector separation of 2.5 cm. The instrument response function (IRF) has been acquired by aligning the tips of source fiber with the detector bundle with a diffusing paper layer in between. After background subtraction, in order to retrieve the absorption and reduced scattering coefficients (μ_a and μ_s'), we have fitted the measured DTOF with the convolution of the solution of the diffusion equation for a semi-infinite medium (with extrapolated boundary conditions) with the IRF. The fitting interval ranges from approximately the 80% of the maximum of the curve on the rising edge to roughly the 0.1% of the maximum for the decaying tails. The measurements have been performed at a room temperature of (25 ± 2) °C.

3. Results and discussion

3.1. Time-resolved spectroscopy results

As explained above, time-resolved spectroscopy measures the time-of-flight of short pulses through the sample. By fitting the measured curves by the use of the diffusion theory, it is possible to determine the optical properties of the phantoms reported in section 2.1. For each concentration of scatterers and glycerol, we have retrieved the reduced scattering coefficient μ_s' and the absorption coefficient μ_a. As for the TRS, in the following we will report only results from the experiments performed at POLIMI, where a multi-wavelength analysis has been performed and where the linear method described in Ref. [38] has been exploited for retrieving the reduced scattering coefficients. As a matter of fact, the use of this method ensures a better accuracy of the retrieved values.

Figure 1(a) shows examples of the retrieved reduced scattering coefficients for varying scatterer concentration for solutions with different glycerol concentration (0%, 10%, 20% and 30%). As expected from theory and previous studies [9–11, 27], for a fixed glycerol concentration, the scattering coefficient increases linearly with the scatterer concentration. We also report fits performed with the equation 2. For the data fitting we have excluded the lowest concentrations of scatterers, since, as previously commented, at that concentrations the validity of diffusion approximation used to retrieve the optical properties is questionable. Detailed results of the fits are reported in Table 1, Section 3.3.

Figure 1(a), furthermore, highlights that the scattering strength of the phantoms depends on the glycerol concentration. This effect is analyzed in Figure 1(b) where we show the fitted intrinsic scattering coefficient (see eq. 2) for the all concentrations of glycerol at three different wavelengths together with the linear fits performed using equation 3. The experimental data show a good agreement with the theory confirming that the scattering properties of the liquid phantoms are changed by adding glycerol to the solution. Detailed results of the linear fits are reported in Table 2, Section 3.3.

The experiments highlight the dependence of the scattering on the wavelength of light. In Figure 1(c), we report the fitted intrinsic scattering coefficient for varying wavelengths at different

Biomedical Optics EXPRESS

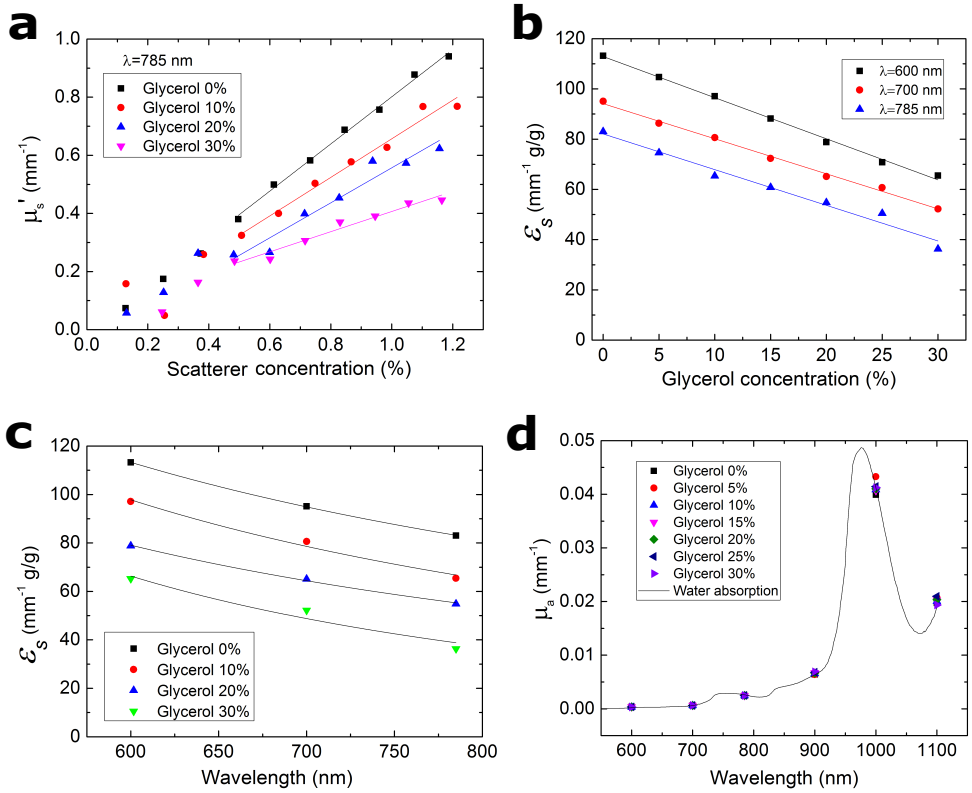

Fig. 1. In panel (a) the reduced scattering coefficient (μ_s') at $\lambda = 785\ nm$ as a function of scatterer concentration at different glycerol concentrations is shown. The dots represent the reduced scattering coefficient measured and the lines the corresponding linear fit. In this case, we have excluded data from the lowest concentrations of scatterers since at such low values of reduced scattering coefficient the diffusion theory is not valid. In panel (b), the intrinsic reduced scattering coefficient of Lipofundin (ϵ_s) for varying glycerol concentrations is shown for three wavelengths. Lines represent the linear fits performed. In panel (c), the intrinsic reduced scattering coefficient of Lipofundin (ϵ_s) for varying wavelengths and different glycerol concentrations is shown. Lines represent the fits performed using the empirical Mie relation (equation 4). Finally, in panel (d), the absorption coefficient (μ_a) spectrum at a fixed scatterer concentration is shown over wavelength. Different colored dots correspond to different glycerol concentrations. The measurements are overlapped with the water absorption spectrum (line). Please note that the concentrations reported in the x-axes of panels (a) and (b) are expressed in % (normalized to 100), while, when reporting the results of the fits in Section 3.3, the concentrations are reported for consistence with literature in g/g (normalized to 1).

glycerol concentrations. The graph shows how the scattering coefficient of the phantom is smaller for longer wavelengths. The results of the fits performed with the empirical Mie relation (equation 4) [12, 34] for different glycerol concentrations are reported in Table 3, Section 3.3.

The TRS measurements allowed, furthermore, the determination of the absorption coefficient μ_a of the system. An example of the absorption coefficient spectrum for different glycerol concentration and fixed scatterer concentration is reported in Figure 1(d) together with the absorption spectrum of the water. The measurements demonstrate that the absorption does not change significantly when the concentration of scatterers and glycerol in the solution changes.

Biomedical Optics EXPRESS

Moreover, Figure 1(d) highlights how the absorption coefficient of the solutions investigated reflects the water absorption. These results demonstrate that the absorption in liquid phantoms made of water/glycerol solutions with Lipofundin as the scattering element can be tuned independently from the scattering and dynamic properties by adding ink or other absorbers to the solution as described in several works [27].

3.2. Diffuse correlation spectroscopy results

The Brownian motion of the scatterers in the phantoms is measured through diffuse correlation spectroscopy experiments performed at ICFO. We have measured phantoms with three different concentrations of glycerol while tuning the reduced scattering coefficient by adding Lipofundin to the initial solution. As explained in Section 2.1, we have tuned the concentration of scatterers in order to obtain approximately the same reduced scattering coefficients (0.5 mm^{-1}, 1 mm^{-1} and 1.5 mm^{-1}) for phantoms with different glycerol concentrations. Table 4 Section 3.3 reports the measured D_b together with the comparison with theory (equation 6) considering the values of viscosity of water/glycerol solutions reported in the literature [25]. A summary of the results obtained is furthermore shown in Figure 2 where we report the ratios of D_b measured for 20% and 30% glycerol solution with D_b measured for solutions with no glycerol. The measured D_b show a clear decrease as the glycerol concentration increases as expected and is in good agreement with the prediction of the theory [18, 25]. Moreover, for the concentration of Lipofundin considered in the experiments D_b resulted independent from the concentration of scatterers in the solutions demonstrating that for such low concentrations Lipofundin does not alter the viscosity of the solutions. The results, furthermore, highlight good reproducibility in the measurements showing only small drifts well within the noise in the measured D_b related to the two different experiments.

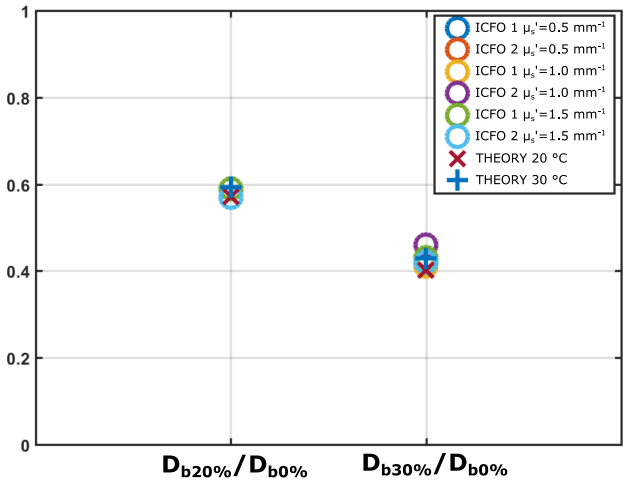

Fig. 2. Results of the two independent DCS experiments (ICFO 1 and ICFO 2) for different glycerol and scatterer concentrations. Detailed results are reported in Table 4, Section 3.3.

3.3. Tables of results and phantom recipe

In this section, we report for completeness a summary of the results obtained through TRS and DCS measurements in different experiments, performed at *Politecnico di Milano* and at *ICFO* together with a practical, explicit phantom recipe.

Biomedical Optics EXPRESS

Tables below show detailed results from all the experiments. Table 1 reports the results of the fits of the reduced scattering coefficient (μ_s') for varying scatterer concentrations (ρ_s), using equation 2. Table 2 reports the results of the fits of the intrinsic scattering coefficient (ϵ_s) for varying glycerol concentration (ρ_{glyc}). Please note that, differently from Figure 1 (a) and (b) where concentrations are reported in % (normalized to 100), here, for consistence with the literature, the results of the fits are reported considering concentrations in g/g (mass of the solid scatterers divided by the mass of the whole solution). Table 3 reports the results of the fits of the intrinsic reduced scattering coefficient (ϵ_s) for varying wavelength using the empirical Mie relation (equation 4) at different glycerol concentrations. Table 4 reports the results of the DCS experiments performed, at different scatterer and glycerol concentrations, together with the expectations from theory (equation 6).

These results provide the basis for a recipe to produce phantoms with the desired optical and dynamic properties. The dynamic properties of the phantom are set considering equation 6 and the viscosity of water/glycerol solutions present in the literature [25]. The results reported in Table 1 can be directly used to set the optical properties of the phantom using equation 2. This provides us with a recipe limited to the glycerol concentrations (0%, 5%, 10%, 15%, 20%, 25%, 30%) and wavelengths (600, 700 and 785 *nm*) that were investigated in our experiments. The extension of the recipe to other glycerol concentrations in water is obtained combining equations 2 and 3, which results in:

$$\rho_s = \frac{\mu_s' - C}{\epsilon_{glyc}\rho_{glyc} + \epsilon_s^0}\,. \tag{7}$$

This equation allows the determination of the concentration of scatterers that have to be inserted in the solution of water and glycerol in order to obtain the desired reduced scattering coefficient for a given wavelength. We note here that, considering the common tissue scattering properties [39], the correction introduced by the coefficient C is negligible considering the experimental errors. A more general phantom recipe considering the wavelength dependence of the reduced scattering coefficient, can be obtained with a deeper analysis of the results reported in Table 3. As expected, the coefficient A scales linearly as the glycerol concentration in the solution increases as

$$A = m\rho_{glyc} + A^0, \tag{8}$$

where m is the slope, ρ_{glyc} is the concentration of glycerol, and A^0 is the intercept, i. e. the value of A for solution with no glycerol. Performing a linear fit we obtain $A^0 = (82.1 \pm 1.4)\ mm^{-1}g/g$ and $m = (-136.4 \pm 8.0)\ mm^{-1}$. Furthermore, the exponent b that depends on the size of the scattering particles is shown to be independent of glycerol concentration. For the purpose of developing a recipe for phantoms we can consider the average of the values reported in Table 3, $b = 1.39 \pm 0.61$. Finally, equations 2, 4 and 8 can be combined to obtain the most general form of the phantom recipe as

$$\rho_s = \frac{\mu_s' - C}{\left(m\rho_{glyc} + A^0\right)\left(\frac{\lambda}{\lambda_0}\right)^{-b}}. \tag{9}$$

where, as already mentioned, the correction introduced by the coefficient C is negligible considering the experimental errors, and C can be considered equal to zero for the purposes of developing tissue mimicking phantoms. Equation 9 is the most general formula for developing phantoms based on water/glycerol solutions and considers both the changes in the bulk refractive index due to the addition of glycerol as well as the wavelength dependence of the optical properties.

Biomedical Optics EXPRESS

Table 1. Results of the fits performed considering equation 2, from the experiment performed at Politecnico di Milano. Error bars are the standard errors of the regressions.

Wavelength (nm)	ϵ_s ($mm^{-1}g/g$)	C (mm^{-1})	Glycerol conc. (%)
600	113.2 ± 2.0	−0.028 ± 0.018	0
700	95.1 ± 1.2	−0.043 ± 0.011	0
785	83.0 ± 1.4	−0.029 ± 0.011	0
600	104.7 ± 2.0	−0.024 ± 0.018	5
700	86.3 ± 1.5	−0.021 ± 0.014	5
785	74.6 ± 1.9	0.011 ± 0.017	5
600	97.1 ± 2.0	−0.041 ± 0.017	10
700	80.6 ± 1.9	−0.054 ± 0.017	10
785	65.4 ± 3.7	−0.003 ± 0.033	10
600	88.2 ± 0.9	−0.024 ± 0.008	15
700	72.3 ± 3.0	−0.039 ± 0.026	15
785	60.8 ± 4.0	0.001 ± 0.033	15
600	78.8 ± 1.4	−0.027 ± 0.012	20
700	65.1 ± 2.3	−0.036 ± 0.020	20
785	54.8 ± 4.6	0.008 ± 0.038	20
600	70.8 ± 2.7	−0.048 ± 0.024	25
700	60.7 ± 2.3	−0.071 ± 0.020	25
785	50.5 ± 1.6	−0.020 ± 0.022	25
600	65.3 ± 1.3	−0.077 ± 0.012	30
700	52.2 ± 1.7	−0.055 ± 0.015	30
785	36.3 ± 2.4	0.044 ± 0.020	30

Table 2. Results of the fits performed considering equation 3, from the experiment performed at Politecnico di Milano. Error bars are the standard errors of the regressions.

Wavelength (nm)	ϵ_{glyc} ($mm^{-1}g/g$)	ϵ_s^0 ($mm^{-1}g/g$)
600	−164 ± 4	112.9 ± 0.8
700	−140 ± 4	94.1 ± 0.7
785	−142 ± 9	82.1 ± 1.8

Biomedical Optics EXPRESS

Table 3. Results of the fits performed using the empirical Mie relation (equation 4) on the data obtained from the experiment performed in Politecnico di Milano. Error bars are the standard errors of the regressions.

Glycerol conc. (%)	A $(mm^{-1}g/g)$	b	λ_0 (nm)
0	83.16 ± 0.22	1.15 ± 0.01	785
5	74.67 ± 0.07	1.26 ± 0.01	785
10	66.8 ± 2.1	1.42 ± 0.16	785
15	61.25 ± 0.66	1.37 ± 0.06	785
20	55.31 ± 0.73	1.33 ± 0.07	785
25	51.5 ± 1.6	1.21 ± 0.16	785
30	38.8 ± 3.6	2.00 ± 0.45	785

Table 4. Results of the DCS experiments are shown. The table reports the measured values of the Brownian diffusion coefficient, D_b, for phantoms with different glycerol and scatterer concentrations. The ratio of the viscosity η is reported for temperature of 20 °C and, in parenthesis, for 30 °C. Error bars are the standard deviations of the results obtained from the four different acquisition channels.

Glycerol conc. (%)	Scatterer conc. (%)	D_b $(10^{-8}cm^2/s)$	μ_s' (mm^{-1})	$D_b/D_{b0\%}$	$\eta_{0\%}/\eta$	Experiment
0	0.75	1.60 ± 0.02	0.5			ICFO 1
0	0.75	1.81 ± 0.03	0.5			ICFO 2
0	1.54	1.68 ± 0.02	1.0			ICFO 1
0	1.54	1.74 ± 0.02	1.0			ICFO 2
0	2.30	1.67 ± 0.04	1.5			ICFO 1
0	2.30	1.76 ± 0.02	1.5			ICFO 2
20	0.89	0.918 ± 0.006	0.5	0.57	0.571 (0.593)	ICFO 1
20	0.89	NA	0.5	NA	0.571 (0.593)	ICFO 2
20	1.80	0.965 ± 0.007	1.0	0.57	0.571 (0.593)	ICFO 1
20	1.80	1.03 ± 0.01	1.0	0.59	0.571 (0.593)	ICFO 2
20	2.72	0.989 ± 0.010	1.5	0.59	0.571 (0.593)	ICFO 1
20	2.72	1.01 ± 0.01	1.5	0.57	0.571 (0.593)	ICFO 2
30	1.22	0.684 ± 0.004	0.5	0.43	0.402 (0.428)	ICFO 1
30	1.22	0.836 ± 0.006	0.5	0.46	0.402 (0.428)	ICFO 2
30	2.64	0.722 ± 0.012	1.0	0.43	0.402 (0.428)	ICFO 1
30	2.64	0.747 ± 0.011	1.0	0.43	0.402 (0.428)	ICFO 2
30	4.04	0.683 ± 0.013	1.5	0.41	0.402 (0.428)	ICFO 1
30	4.04	0.730 ± 0.006	1.5	0.42	0.402 (0.428)	ICFO 2

Biomedical Optics EXPRESS

4. Conclusion

In conclusion, we have designed and prepared liquid phantoms consisting on solutions of water and glycerol with Lipofundin as the scattering element. The phantoms produced have well defined optical and dynamic properties and have been characterized through TRS and DCS measurements. The experiments allowed us to provide a practical recipe to prepare liquid phantoms. By tuning the glycerol concentration in water it is possible to control the viscosity of the solution, i. e. tuning the Brownian diffusion of the scatterers. Then, for fixed concentrations of glycerol, we have stated the recipe to obtain the desired scattering properties, adding Lipofundin to the solution.

Funding

European Union's Horizon 2020 research and innovation programme (LUCA-project, No. 688303) as an initiative of the Photonics Public Private Partnership; Fundació CELLEX Barcelona; Ministerio de Economía y Competitividad / FEDER (PHOTODEMENTIA, DPI2015-64358-C2-1-R); Instituto de Salud Carlos III / FEDER (MEDPHOTAGE, DTS16/00087); the "Severo Ochoa" Programme for Centres of Excellence in R&D (SEV-2015-0522); the Obra social "la Caixa" Foundation (LlumMedBcn); AGAUR-Generalitat (2014SGR-1555); European Union - Competitiveness and Innovation Framework Programme 2007-2013 (BabyLux, 620996 CIP-ICT-PSP-2013-7); LASERLAB-EUROPE IV.

Acknowledgments

The authors would like to thank M. Kacprzak for the support in setting up the ICFO experiments.

Disclosures

ICFO has equity ownership in the spin-off company HemoPhotonics S.L.. Udo Weigel is the CEO, has equity ownership and is an employee of the company. Potential financial conflicts of interest and objectivity of research have been monitored by ICFO's Knowledge & Technology Transfer Department. No financial conflicts of interest were identified.